

# Global Analysis of Solar Neutrino Oscillations Including SNO CC Measurement

---

**John N. Bahcall**

*School of Natural Sciences, Institute for Advanced Study, Princeton, NJ 08540*

*E-mail: jnb@ias.edu*

**M. C. Gonzalez-Garcia**

*Theory Division, CERN, CH-1211, Geneva 23, Switzerland*

*E-mail: concha@thwgs.cern.ch*

*and Instituto de Física Corpuscular, Universitat de València – C.S.I.C. Edificio*

*Institutos de Paterna, Apt 22085, 46071 València, Spain*

**Carlos Peña-Garay**

*Instituto de Física Corpuscular, Universitat de València – C.S.I.C. Edificio*

*Institutos de Paterna, Apt 22085, 46071 València, Spain*

*penya@ific.uv.es*

**ABSTRACT:** For active and sterile neutrinos, we present the globally allowed solutions for two neutrino oscillations. We include the SNO CC measurement and all other relevant solar neutrino and reactor data. Five active neutrino oscillation solutions (LMA, LOW, SMA, VAC, and Just  $So^2$ ) are currently allowed at  $3\sigma$ ; three sterile neutrino solutions (Just  $So^2$ , SMA, and VAC) are allowed at  $3\sigma$ . The goodness of fit is satisfactory for all eight solutions. We also investigate the robustness of the allowed solutions by carrying out global analyses with and without: 1) imposing solar model constraints on the  $^8B$  neutrino flux, 2) including the Super-Kamiokande spectral energy distribution and day-night data, 3) using an enhanced CC cross section for deuterium (due to radiative corrections), and 4) a optimistic, hypothetical reduction by a factor of three of the error of the SNO CC rate. For every analysis strategy used in this paper, the most favored solutions all involve large mixing angles: LMA, LOW, or VAC. The favored solutions are robust, but the presence at  $3\sigma$  of individual sterile solutions and the active Just  $So^2$  solution is sensitive to the analysis assumptions.

**KEYWORDS:** solar and atmospheric neutrinos, neutrino and gamma astronomy, neutrino physics.

---

## Contents

1. Introduction	1
2. Calculational Procedures	2
3. Global Solutions including Rates and Day-Night Spectra	4
4. Rates-only Global Solutions	10
5. Discussion	13

---

## 1. Introduction

The epochal Sudbury Neutrino Observatory (SNO) measurement [1] of the CC rate for solar neutrino absorption by deuterium provides an important new constraint on the allowed neutrino oscillation solutions. We present in this paper solutions for the globally allowed regions that include, in addition to the SNO CC measurement, the available data from the Chlorine [2], Gallium [3, 4, 5], and Super-Kamiokande [6] experiments.

We also explore the robustness of the global solutions to different analysis strategies.

The most radical test we make is to determine the allowed solutions if only the total rates of the solar neutrino experiments are used, ignoring the beautiful data from the Super-Kamiokande measurements of the spectral energy distribution and the day-night variations. This test is motivated by the fact that the Super-Kamiokande day and night recoil energy spectra provide 38 different data points, while the rates of the chlorine experiment, the two gallium experiments, and SNO provide together only 4 data points. Some authors have questioned whether  $\chi^2$  fits to the complete data set overweight the Super-Kamiokande data because of the large number of spectral energy bins [7].

We take both sides of the somewhat philosophical question of whether the  ${}^8\text{B}$  neutrino flux should be allowed to vary without considering constraints from the solar model. We find self-consistent global solutions both with and without imposing the solar model constraints.

We require (cf. [8]) that the  ${}^8\text{B}$  neutrino flux be treated the same way in all aspects of the calculation, either completely free when evaluating both the rates and

the energy spectrum or constrained everywhere by the solar model predictions. We also require that the  ${}^8\text{B}$  neutrino flux be identical in all parts of the calculation. Finally, we avoid double counting the SuperKamiokande rate measurement; we do not include the measured flux normalization both in the rate measurement and in the spectral energy distribution. Many other analyses do not satisfy these requirements.

Why do all these tests? There are not yet enough solar neutrino experiments to ensure cross checks and redundancy in the data. Therefore, different plausible analysis schemes can lead to different conclusions. The existence of a particular allowed region, e. g., the SMA solution or the Just  $\text{So}^2$  solution, may depend upon which of several possible plausible analysis schemes are used. Our motto is: “If its not robust, its not believable.”

In Section 2, we summarize the calculational procedures. Because of the excellent agreement between the predicted standard solar model flux of  ${}^8\text{B}$  neutrinos (see ref. [9], BP00) and the combined SNO [1] and Super-Kamiokande [6] measurement, we include the theoretical fluxes and their BP00 uncertainties in our standard analysis. We also use a ‘level playing field’ prescription for evaluating the allowed active and sterile neutrino solutions. We present in Section 3 the allowed solutions that exist if all the solar neutrino data, including the spectral energy distribution and day night data of Super-Kamiokande, are included in the analysis. Considering only the total rates in the chlorine, gallium, Super-Kamiokande, and SNO experiments, we present in Section 4 the allowed solutions for this extreme case. We also investigate the effects of allowing the  ${}^8\text{B}$  flux to vary unconstrained by solar model predictions, of using a larger CC cross section for deuterium (motivated by possible effects of radiative corrections [10]), and of a hypothetical reduction by a factor of three in the total quoted error for the SNO CC rate. We summarize our results in Section 5.

## 2. Calculational Procedures

We use, unless stated otherwise, the techniques and parameters for the analysis that we have described elsewhere [8] and [11].

Once the SNO results are included in the analysis, all of the solutions with sterile neutrinos are relatively poor fits to the totality of solar neutrino data. Many different regions of the sterile neutrino parameter space provide comparable fits to the available data. We have therefore made one significant departure from previous analysis techniques for two neutrino oscillations: we treat the active and sterile neutrinos as different aspects of the same two-neutrino oscillation scheme. This procedure ‘levels the playing field’ for active and sterile neutrinos. The assumption of oscillation into either all active or all sterile neutrinos describes the limiting extremes of a continuum in which the oscillation occurs into a linear combination of active and sterile neutrinos, see discussion in ref. [12] of four neutrino oscillations.

Our theoretical framework contains three free parameters:  $\Delta m^2$ ,  $\tan^2 \theta$ , and the third parameter,  $\cos^2 \eta$ , which defines the active-sterile admixture. We focus here only on the two limiting cases,  $\cos^2 \eta = 1, 0$ . Since the parameter space is three-dimensional, the allowed regions for a given C.L. are defined as the set of points satisfying the condition

$$\chi_{\text{sol}}^2(\Delta m^2, \theta, \eta) - \chi_{\text{sol,min}}^2 \leq \Delta \chi^2(\text{C.L., 3 d.o.f.}), \quad (2.1)$$

where  $\Delta \chi^2(\text{C.L., 3 d.o.f.}) = 6.25, 7.81, 11.34$ , and  $14.16$  for C.L. = 90%, 95%, 99% and 99.73% ( $3\sigma$ ) respectively, and  $\chi_{\text{sol,min}}^2$  is the global minimum in the three-dimensional space. Following Fogli, Lisi, and Montanino [13] and de Gouvea, Friedland, and Murayama [14], we present our results in terms of  $\tan^2 \theta$  rather than  $\sin^2 2\theta$  in order to include solutions with mixing angles greater than  $\pi/4$  (the so-called ‘dark side’).

In our statistical treatment of the data, we follow the analysis of ref. [15], with the updated uncertainties and distributions for neutrino production fractions and the solar matter density given in ref. [9] and tabulated in <http://www.sns.ias.edu/~jnb>.

In Section 3, we determine the allowed range of the oscillation parameters using the CC event rate measured at SNO, the Chlorine and Gallium event rates (we use here the weighted averaged GALLEX/GNO and SAGE rates), and the  $2 \times 19$  bins of the Super-Kamiokande electron recoil energy spectrum measured separately during the day and night periods. In this global analysis we adopt the prescription described in ref. [8]. We do not include here the Super-Kamiokande total rate, since to a large extent the total rate is represented by the flux in each of the spectral energy bins. We define the  $\chi^2$  function for the global analysis as:

$$\chi_{\text{global}}^2 = \sum_{i,j=1,41} (R_i^{\text{th}} - R_i^{\text{exp}}) \sigma_{G,ij}^{-2} (R_j^{\text{th}} - R_j^{\text{exp}}) \quad (2.2)$$

where  $\sigma_{G,ij}^2 = \sigma_{R,ij}^2 + \sigma_{Sp,ij}^2$ . Here  $\sigma_{R,ij}$  is the corresponding  $41 \times 41$  error matrix containing the theoretical as well as the experimental statistical and systematic uncorrelated errors for the 41 rates while  $\sigma_{Sp,ij}$  contains the assumed fully-correlated systematic errors for the  $38 \times 38$  submatrix corresponding to the Super-Kamiokande day-night spectrum data. We include here the energy independent systematic error which is usually quoted as part of the systematic error of the total rate. The error matrix  $\sigma_{R,ij}$  includes important correlations arising from the theoretical errors of the solar neutrino fluxes, or equivalently of the solar model parameters.

When considering just the total rates (see Section 4), we adapt the  $\chi^2$  definition of ref. [15, 16] to include the two different gallium rates and the new SNO CC event rate. The  $\chi^2$  for this case is

$$\chi_{\text{Rates}}^2 = \sum_{i,j=1,5} (R_i^{\text{th}} - R_i^{\text{exp}}) \sigma_{R,ij}^{-2} (R_j^{\text{th}} - R_j^{\text{exp}}), \quad (2.3)$$

where  $R_i^{th}$  is the theoretical prediction of the event rate in detector  $i$  and  $R_i^{exp}$  is the measured rate. The error matrix  $\sigma_{ij}$  contains the experimental errors, both systematic and statistical, as well as the theoretical uncertainties on the solar neutrino fluxes and the interaction cross sections. The theoretical error matrix includes important correlations arising from the theoretical errors of the solar neutrino fluxes, or equivalently of the solar model parameters. Furthermore for the GALLEX/GNO and SAGE rates, the corresponding theoretical errors for the interaction cross section are assumed to be fully correlated.

One of the largest systematic uncertainties in interpreting the SNO CC measurement results from the uncertainty in the absolute value of the neutrino absorption cross section on deuterium [1, 17]. We have used in our calculations the cross sections calculated by Nakamura et al. [18], which are in good agreement with the results of Butler et al. [19]. Most recently, Beacon and Parke [10] have argued that there may be a 6% increase in the cross sections evaluated by Nakamura et al and Butler et al. due to a combination of factors represented by a 2% correction to  $g_A^2$ , and two other factors related to radiative corrections [20]. We follow the SNO collaboration [1, 21] in including the 2% correction from  $g_A^2$  in our standard calculations.

In order to test the sensitivity of the global fits to the effects of radiative corrections, we have repeated all of our calculations with a CC cross section for SNO that is increased by an additional 4% relative to the standard cross sections. We shall describe these calculations in the text as having been done with the 'enhanced CC cross sections.'

For the SNO CC calculation, we have used the resolution function given in ref. [1], which is slightly broader than we have assumed in our previous analyses.

### 3. Global Solutions including Rates and Day-Night Spectra

We describe in this section global solutions obtained by using all the relevant solar neutrino and reactor data.

Figure 1 shows the globally allowed solutions when the Super-Kamiokande recoil energy spectrum during the day and, separately, the energy spectrum at night are included in addition to the total rates in the Chlorine [2], Gallium (averaged) [3, 5, 4], and SNO [1] experiments. In order to avoid double counting the Super-Kamiokande total rate(cf. ref. [8] for a discussion of this point), we have not included the Super-Kamiokande rate [6] in addition to the Super-Kamiokande day and night energy spectra, which each contain their own absolute normalizations. We have used the Chooz reactor bound [22] to cutoff the allowed solutions slightly below  $10^{-3}$  eV<sup>2</sup>.

Figure 1 is our currently preferred global solution.

All eight of the allowed solutions for active and sterile neutrinos that existed before the SNO CC measurement (e.g., ref. [8]) are still allowed at  $3\sigma$  after including the results of the SNO CC measurement.

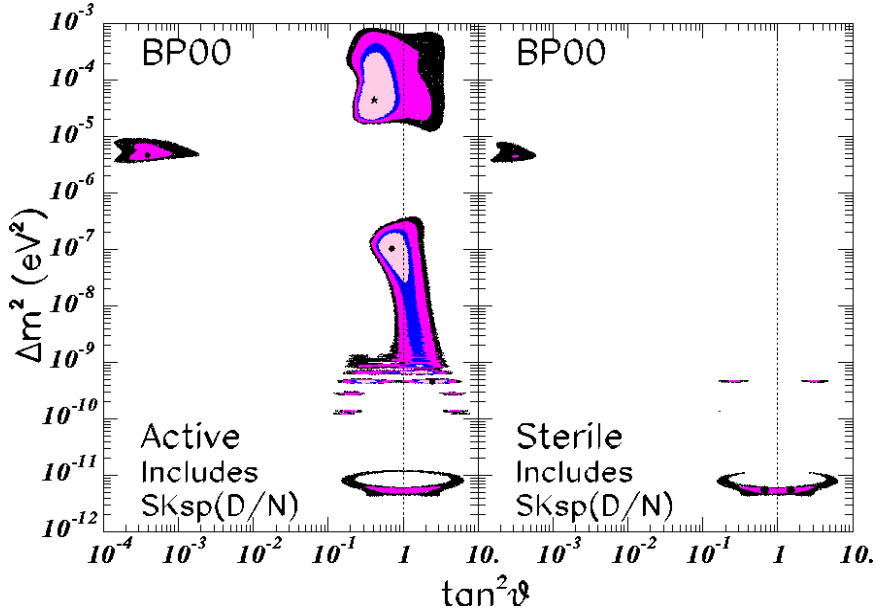


**Figure 1: Global solutions including all available solar neutrino data.** The input data include the total rates from the Chlorine [2], Gallium (averaged) [3, 5, 4], Super-Kamiokande [6], and SNO [1] experiments, as well as the recoil electron energy spectrum measured by Super-Kamiokande during the day and separately the energy spectrum measured at night. The C.L. contours shown in the figure are 90%, 95%, 99%, and 99.73% ( $3\sigma$ ). The allowed regions are cutoff below  $10^{-3}\text{eV}^2$  by the Chooz reactor measurements [22]. The local best-fit points are marked by dark circles. The theoretical errors for the BP2000 neutrino fluxes are included in the analysis.

Table 1 gives the best-fit parameters for each of the eight allowed oscillation solutions illustrated in Figure 1. We give in Table 1 the values of  $\Delta m^2$ ,  $\tan^2 \theta$ ,  $\chi^2_{\min}$ , and the goodness-of-fit for each of the best-fit points. The solutions described by the acronyms like LMA and Just So<sup>2</sup> can be identified in Figure 1 with the aid of Table 1 by using the association between the solution acronyms (column 1) and the values of  $\Delta m^2$  (column 2).

The LMA active solution is the best-fit, but is only slightly better than the LOW and VAC active solutions. The SMA solution is a significantly less good fit than the LMA and LOW solutions. The goodness-of-fit ranges from 59% for the LMA active solution to 15% for the Sterile VAC solution, all satisfactory fits to the available data.

The five active solutions, LMA, SMA, LOW, VAC, and Just So<sup>2</sup> all appear clearly in the left hand panel of Figure 1, although the allowed area of the SMA solution has shrunk significantly relative to the pre-SNO situation (cf. refs. [8, 11]).<sup>1</sup>

<sup>1</sup>We caution the reader that the comparison with previous results is not entirely straightforward since we have included in the  $\chi^2$  analysis an additional parameter ( $\cos \eta = 1, 0$ , for active or sterile

Solution	$\Delta m^2$	$\tan^2(\theta)$	$\chi^2_{\min}$	g.o.f.
LMA	$4.5 \times 10^{-5}$	$4.1 \times 10^{-1}$	35.3	59%
LOW	$1.0 \times 10^{-7}$	$7.1 \times 10^{-1}$	38.4	45%
VAC	$4.6 \times 10^{-10}$	$2.4 \times 10^0$	39.0	42%
SMA	$4.7 \times 10^{-6}$	$3.9 \times 10^{-4}$	45.4	19%
Just So <sup>2</sup>	$5.5 \times 10^{-12}$	$0.67(1.5) \times 10^0$	45.7	18%
Sterile Just So <sup>2</sup>	$5.5 \times 10^{-12}$	$0.67(1.5) \times 10^0$	45.8	18%
Sterile SMA	$4.5 \times 10^{-6}$	$3.1 \times 10^{-4}$	46.6	16%
Sterile VAC	$4.7 \times 10^{-10}$	$2.7 \times 10^{-1}$	47.2	15%

**Table 1: Best-fit global oscillation parameters with all solar neutrino data.**

This table corresponds to the global solution illustrated in Figure 1. The differences of the squared masses are given in eV<sup>2</sup>. The number of degrees of freedom is 38 [38(spectrum) + 3(rates) − 3(parameters:  $\Delta m^2$ ,  $\theta$ , active–sterile admixture)]. The goodness-of-fit given in the last column is calculated using the value of  $\chi^2/d.o.f$  for each allowed solution. The BP00 best-fit fluxes and their estimated errors have been included in the analysis. The rates from the GALLEX/GNO and SAGE experiments have been averaged to provide a unique data point. The goodness-of-fit given in the last column is calculated from the value of  $\chi^2/d.o.f$  at each local minimum (i. e., for LMA, SMA, VAC, LOW, etc.).

The largest reduction in allowed area occurs for the Sterile SMA, which is barely visible at  $3\sigma$  C.L. in the right hand panel of Figure 1. The other sterile solutions are not much affected at  $3\sigma$  by the SNO CC measurement, although they have also become somewhat less likely.

We can learn something very instructive about the existence or non-existence of the SMA solutions from a variation on this analysis scheme. The relative quality of both the active and the sterile SMA solutions with respect to the active LMA solution is slightly dependent on the way the normalization of the SuperKamiokande total rate is included in the analysis. If we include in the analysis the SuperKamiokande total event rate but allow a free normalization for the SuperKamiokande day and night energy spectra, we obtain a relatively worse g.o.f. for the SMA solutions while the g.o.f. of the LMA solution is essentially unchanged ( $\chi^2_{\text{LMA}} = 35.5$ ,  $\chi^2_{\text{SMA}} = 49.8$ ,  $\chi^2_{\text{sterile SMA}} = 53.4$ ). As a consequence, the active and sterile SMA solutions do not appear at the  $3\sigma$  level in such an analysis. We trace the origin of this difference to the effect of the energy independent systematic errors. When introduced in the spectrum, as we do in our analysis, even if fully correlated, the energy independent systematic errors result in a slightly smaller correlation among the errors of the different energy bins in the spectrum. As a consequence the spectrum becomes less rigid and allows

neutrinos) and we measure all departures from  $\chi^2_{\min}$ , the best-fit value with either active or sterile neutrinos. We have also made a few minor adjustments in the analysis code.

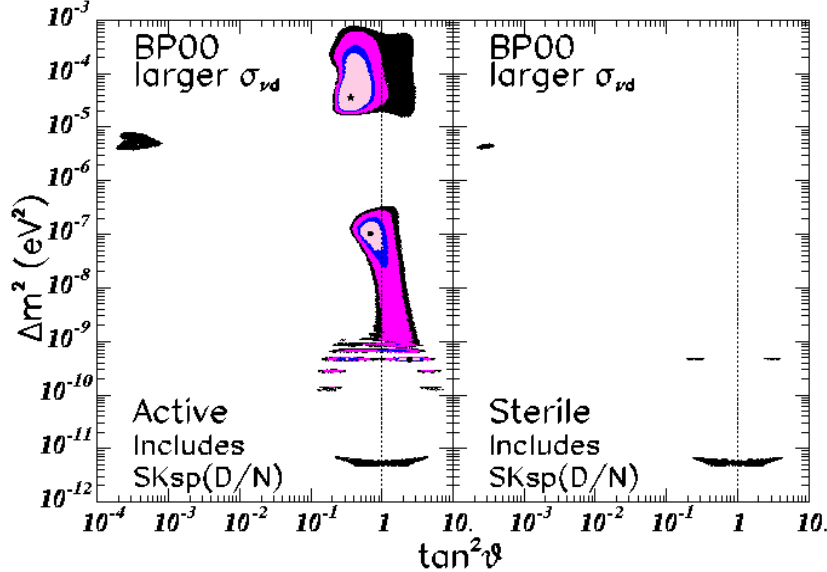


**Figure 2:** Global solutions including all available solar neutrino data, with enhanced CC cross section for deuterium. The input data are the same as in Figure 1 except that we have used a 4% large CC cross section for neutrino absorption on deuterium.

a better fit for the SMA solutions. This is an example where we think it is useful to apply the motto: “If it is not robust, it is not believable.”

Solution	$\Delta m^2$	$\tan^2(\theta)$	$\chi^2_{\min}$	g.o.f.
LMA	$3.7 \times 10^{-5}$	$3.7 \times 10^{-1}$	34.7	62%
LOW	$1.0 \times 10^{-7}$	$6.9 \times 10^{-1}$	39.2	42%
VAC	$4.6 \times 10^{-10}$	$2.4 \times 10^0$	39.7	39%
SMA	$4.6 \times 10^{-6}$	$3.4 \times 10^{-4}$	47.0	15%
Just So <sup>2</sup>	$5.5 \times 10^{-12}$	$0.67(1.5) \times 10^0$	46.8	15%
Sterile Just So <sup>2</sup>	$5.5 \times 10^{-12}$	$0.67(1.5) \times 10^0$	47.0	15%
Sterile SMA	$4.5 \times 10^{-6}$	$2.9 \times 10^{-4}$	48.2	12%
Sterile VAC	$4.7 \times 10^{-10}$	$2.7 \times 10^{-1}$	48.5	12%

**Table 2:** Best-fit global oscillation parameters with an enhanced CC cross section for deuterium, corresponding to Figure 2. The input data used in constructing this table were the same as were used in constructing Table 1 except that for this table we adopted a 4% larger CC cross section for deuterium.

What is the effect of the possibly enhanced cross section discussed in ref. [10] and in Section 2? Figure 2 and Table 2 show the results that are obtained when

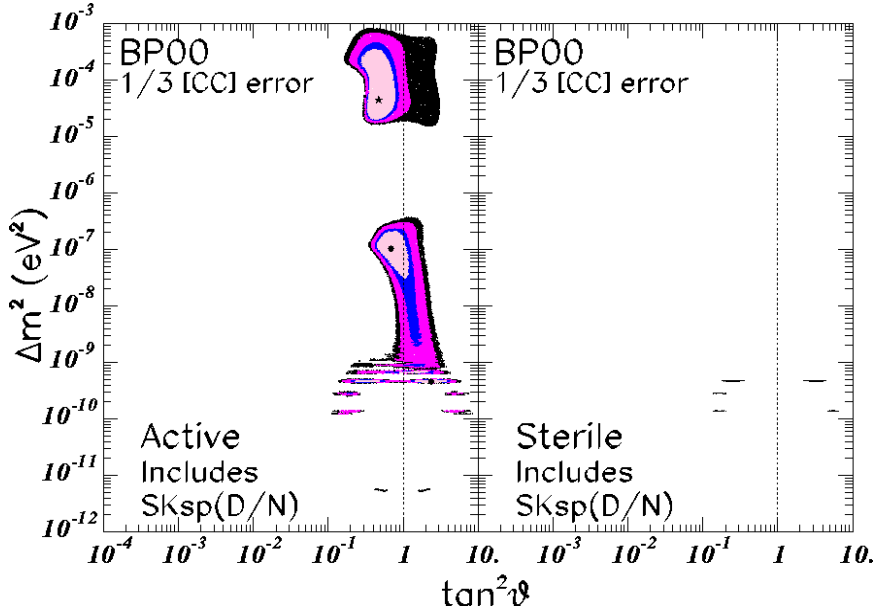


**Figure 3: Global solutions with error on SNO CC flux reduced by a factor of three.** The input data are the same as for Figure 1 except that the error on the  $\nu_e$  flux of  $^8\text{B}$  neutrinos for SNO was artificially reduced by a factor of three.

a CC cross section enhanced by 4% is assumed for deuterium. It is instructive to compare directly Figure 2 and Table 2 with Figure 1 and Table 1. Doing so, we see that no qualitative changes are induced by using the larger CC cross section for deuterium. The main quantitative change is that the allowed regions for the SMA solutions, both active and sterile, become slightly smaller and less statistically likely when the larger CC cross section is assumed. All of the sterile neutrino solutions become slightly less good fits.

The wonderful measurement of the  $\nu_e$  flux of  $^8\text{B}$  neutrinos that has recently been reported by SNO [1] is the first quantitative result reported by this collaboration. It is therefore plausible that the error on the  $\nu_e$  flux will decrease with time as the systematic uncertainties become better understood and the statistical errors are reduced by counting more events. In an uncontrolled burst of optimism, we have hypothesized that the quoted experimental error on the  $\nu_e$  flux will be ultimately reduced by a factor of three while the best-estimate value for the  $\nu_e$  flux will be unchanged.

Figure 3 shows the effect on the globally allowed solutions of reducing the total error on the CC flux measurement of SNO by a factor of three relative to the total error quoted in ref. [1]. Comparing Figure 3 with Figure 1, we see that a factor of three improvement in the quoted error could eliminate at  $3\sigma$  both the active and the sterile SMA solutions and disfavor (rule out at  $3\sigma$ ) the active (sterile) Just So<sup>2</sup>

solution. The allowed LMA and LOW solutions would not be much affected by even a factor of three reduction in the error in the  $\nu_e$  flux, the main effect being a modest reduction of the area of the allowed LMA solution in the  $\Delta m^2$ - $\tan^2 \theta$  plane.

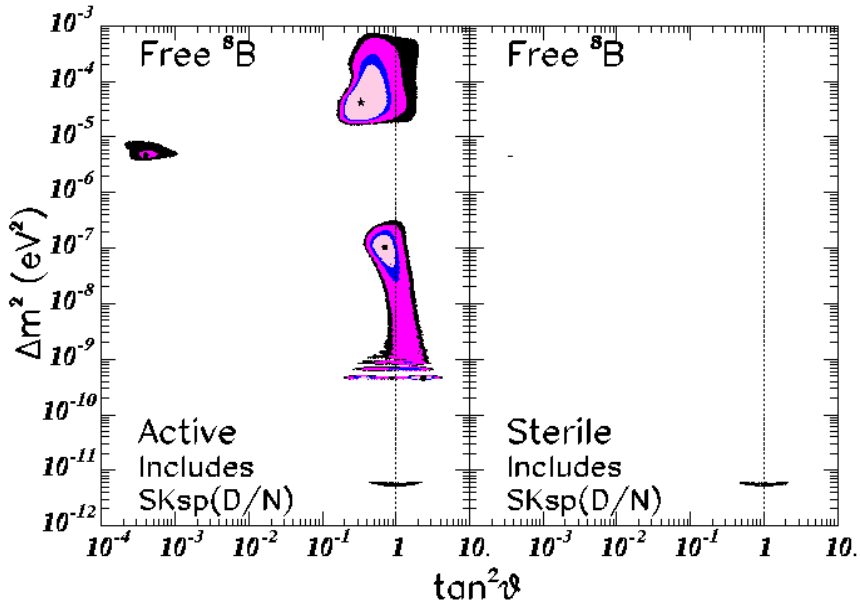


**Figure 4: Global solutions, with unconstrained<sup>8</sup>B neutrino flux, including all available solar neutrino data.** The input data and the analysis are the same as were used in constructing Figure 1 except that for the present figure no constraint was placed on the <sup>8</sup>B neutrino flux.

Does it make a difference if we constrain the <sup>8</sup>B neutrino flux according to the predictions of the standard solar model? This is an important question to answer, since one can give reasonable arguments on both sides of the question as to whether or not it is more appropriate to constrain the <sup>8</sup>B neutrino flux. Arguing in favor, one can point out that the standard solar model provides relevant information about the solar interior and about the rates of solar fusion reactions. Moreover, the standard solar model is remarkably successful in predicting results in agreement with helioseismological measurements [9]. On the other hand, we would like to determine the <sup>8</sup>B neutrino flux independent of solar model considerations. For a model-independent analysis, we must allow the <sup>8</sup>B neutrino flux to vary freely.

Figure 4 shows the result of an analysis that is identical to our standard analysis except that the <sup>8</sup>B neutrino flux was not constrained by solar model predictions. The three most favored solutions all involve large mixing angles; they are (with their associated g.o.f.): LMA (59%), LOW (39%), and VAC (35%). The g.o.f. for all the other solutions is less than 20%.

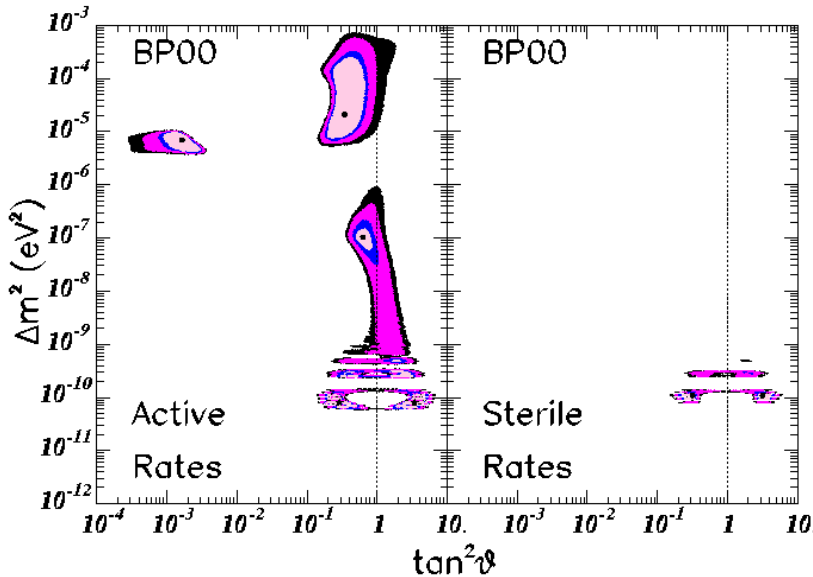


**Figure 5: Global solutions for the rates only.** The input data are the total rates measured in the SNO CC [1], Chlorine [2], SAGE [4] + (GALLEX [3] + GNO [5]), and Super-Kamiokande [6] experiments. The C.L. contours shown in the figure are 90%, 95%, 99%, and 99.73% ( $3\sigma$ ). The local best-fit points are marked by dark circles. The theoretical errors for the BP2000 neutrino fluxes are included in the analysis.

Comparing Figure 4 and Figure 1, we see that the favored, large angle solutions, LMA and LOW, are not changed significantly. However, the allowed regions for the SMA and Just So<sup>2</sup> solutions, both active and sterile, are reduced in size by performing a <sup>8</sup>B-free analysis. The sterile SMA allowed region is reduced to almost a point in Figure 4. To find the sterile SMA in Figure 4, one has to know where to look, namely, near the  $\Delta m^2$  and  $\tan^2\theta$  for which the best-fit SMA solution appears for active neutrinos. Also, the small sterile VAC region that appears in Figure 1 disappears entirely in Figure 4,

It is difficult to anticipate intuitively the quantitative difference between global solutions obtained without and with constraints on the <sup>8</sup>B neutrino flux. This is particularly true for the less robust solutions, like all of the sterile solutions and the Just So<sup>2</sup> active solution. Two factors work in opposite directions in determining  $\chi^2$ : 1) the free normalization in the <sup>8</sup>B neutrino flux; and 2) the removal of the theoretical error in the flux. The second effect seems to be generally more important.

#### 4. Rates-only Global Solutions

We describe in this section global solutions obtained by considering only the total

rates in the Chlorine, GALLEX/GNO, SAGE, Super-Kamiokande, and SNO (CC) solar neutrino experiments. We also evaluate the effects of varying the  ${}^8\text{B}$  neutrino flux unconstrained by solar model predictions and of increasing the CC cross section for SNO.

Figure 5 and Table 3 present the allowed solution regions and the best-fit parameters for the global analysis of only the total rates. The best-fit point is in the VAC region with the LMA solution giving a rather similar  $\chi^2_{\min}$ .

Solution	$\Delta m^2$	$\tan^2(\theta)$	$\chi^2_{\min}$	g.o.f.
VAC	$7.9 \times 10^{-11}$	$0.29(3.45)$	3.50	17%
LMA	$2.1 \times 10^{-5}$	$3.4 \times 10^{-1}$	3.99	14%
SMA	$6.9 \times 10^{-6}$	$1.6 \times 10^{-3}$	5.25	7%
LOW	$9.7 \times 10^{-8}$	$6.5 \times 10^{-1}$	8.61	1.4%
Sterile VAC	$1.1 \times 10^{-10}$	$0.29(3.45)$	10.1	0.63%
Sterile SMA	$4.9 \times 10^{-6}$	$5.3 \times 10^{-4}$	18.0	0.01%

**Table 3: Best-fit parameters for total rates only, corresponding to Figure 5.** The format of this table is the same as for Table 1. The two rates measured by the Gallium experiments, (GALLEX [3] and GNO [5]) and SAGE [4], are included separately. The number of degrees of freedom is 2 [5(rates) – 3(parameters:  $\Delta m^2$ ,  $\theta$ ,  $O$  = active or sterile neutrino)]. The Sterile SMA solution does not appear in Figure 5 because  $\chi^2_{\min}$  is too large for this solution, but the result is given in the table for general information.

For the LMA, SMA, and LOW solutions, the results appear superficially similar to what is obtained when the Super-Kamiokande spectral data for both the day and the night are included in the analysis (cf. Figure 1 and Figure 5). However, the g.o.f. is poorer (cf. Table 1 and Table 3) when the spectral data are included, which reflects the fact that solutions which predict a flat spectrum in the energy region studied by Super-Kamiokande are favored.

The principal changes that result from omitting the spectral and the day-night data are for the vacuum solutions near  $10^{-10}$  eV $^2$ , the Just So $^2$  solution, and the Sterile SMA solution. The vacuum solutions are much more prominent when the spectral data are not considered. This is a well-known effect and has been noted in many previous analyses. The Just So $^2$  solution is missing when only the rates are considered, which is largely due to the imposition of the BP00 theoretical constraint on the  ${}^8\text{B}$  flux [8]. The sterile SMA solution also disappears completely at  $3\sigma$  (just barely, see Table 3).

Figure 6 and Table 4 show that enhancing the CC cross section by 4% has very little effect on the allowed regions when only the data on total event rates is considered. This result is seen most clearly by comparing directly Figure 5 and Table 3 with Figure 6 and Table 4.

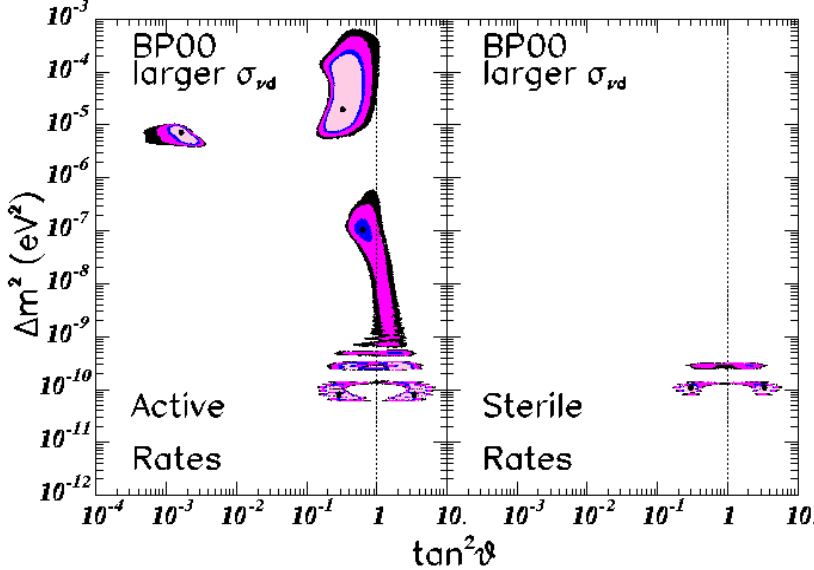


**Figure 6: Global solutions for the rates only, with an enhanced CC cross section for deuterium.** The input data and the analysis procedures are the same as used in producing Figure 5, except that we have used for the present figure a 4% larger CC cross section for neutrino absorption by deuterium.

Solution	$\Delta m^2$	$\tan^2(\theta)$	$\chi^2_{\min}$	g.o.f.
VAC	$7.9 \times 10^{-11}$	$0.29(3.45)$	3.07	21%
LMA	$2.0 \times 10^{-5}$	$3.3 \times 10^{-1}$	3.45	18%
SMA	$7.3 \times 10^{-6}$	$1.6 \times 10^{-3}$	7.09	2.9%
Sterile VAC	$1.1 \times 10^{-10}$	$0.29(3.45)$	9.12	1.1%
LOW	$1.1 \times 10^{-7}$	$6.3 \times 10^{-1}$	9.45	0.89%
Sterile SMA	$4.7 \times 10^{-6}$	$4.6 \times 10^{-4}$	20.7	0.003%

**Table 4: Best-fit parameters for total rates only with enhanced CC cross section for deuterium, corresponding to Figure 6.** The input data for this analysis are the same as for the analysis described by Table 4 except that a 4% larger CC cross section for deuterium was used here.

Figure 7 shows the allowed solutions that are obtained when the  ${}^8\text{B}$  flux is permitted to vary freely, without considering the constraints implied by the standard solar model. The only obvious differences between Figure 7 and Figure 6, for which the  ${}^8\text{B}$  flux was constrained by the BP00 flux predictions, are that the Just  $\text{So}^2$  solutions appear when the flux is allowed to vary freely and the sterile SMA solution is restored at a  $3\sigma$  C.L. Since the Just  $\text{So}^2$  solutions correspond to a  ${}^8\text{B}$  flux that is

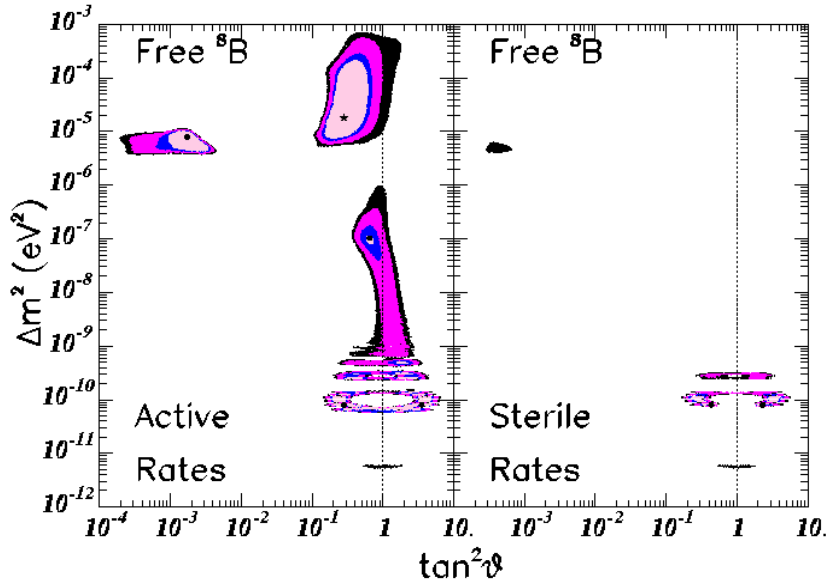


**Figure 7: Global solutions for the rates only, with an unconstrained  ${}^8\text{B}$  neutrino flux.** The input data and the analysis procedures are the same as used in producing Figure 5, except that the  ${}^8\text{B}$  flux is allowed to vary without considering the predicted flux or errors of the standard solar model.

small compared to the BP00 flux ( 0.46 of the BP00 flux, cf. refs. [8, 23, 24]), these solutions are disfavored when the BP00 flux constraints are imposed.

Finally, we have investigated the effect of reducing the total error on the  $\nu_e$  flux measured by SNO. We have supposed, in the same burst of wild optimism that prevailed previously (see Section 3, especially the discussion of Figure 3), that the total error on the  $\nu_e$  flux is reduced by a factor of three while the best-estimate for the flux remains unchanged from the value quoted by ref. [1]. We find results consistent with the discussion of Figure 3, which applies to the case when all the available solar neutrino data are included in the analysis. In the present case, we find that the SMA solution is greatly reduced in area. The LMA and LOW solutions are not qualitatively affected.

## 5. Discussion

Our principal conclusions are simple to state.

First, for every one of the analysis strategies used in this paper, the favored solutions all involve large mixing angles: LMA, LOW, or VAC.

Second, all eight of the previously recognized two component oscillation solutions are still allowed at  $3\sigma$  if one considers in the analysis the solar model constraints on the  ${}^8\text{B}$  neutrino flux and all the available neutrino data, including the SNO CC

measurement and the SuperKamiokande spectral energy distributions in the day and at night. The goodness of fit for all of these solutions ranges from good to satisfactory. The results are shown in Figure 1 and Table 1, which describe the currently preferred global solution.

Third, even the extreme assumption of ignoring all the SuperKamiokande data on the spectral recoil energy distribution and the day-night variations does not change very much the allowed regions of the preferred solutions. Only the marginally allowed Just So<sup>2</sup> active and sterile solutions and the SMA sterile solution are not allowed at  $3\sigma$  when the spectral and day-night data are ignored. This result can be seen by comparing Figure 5 with Figure 1.

Fourth, the global solutions that are obtained with and without solar model constraints on the  $^8\text{B}$  neutrino flux are very similar for the favored large mixing angle solutions. This result can be seen by comparing visually Figure 1 and Figure 4 (both constructed using all the available solar neutrino data) and Figure 6 and Figure 7 (both constructed using only the data on the total rates). The only apparent differences occur for marginally allowed regions like the sterile solutions and the active Just So<sup>2</sup> solution. The reason for the insensitivity to how the  $^8\text{B}$  neutrino flux is treated is that the combined SNO and SuperKamiokande measurement of the total flux [1] is in excellent agreement with the standard solar model prediction [9].

Fifth, the allowed solution space is not qualitatively affected by a suggested [10] increase by 4% of the CC cross section on deuterium, although the allowed regions of the SMA and the Just So<sup>2</sup> solutions become somewhat smaller when the cross section is enhanced. This result can be inferred from a comparison of Figure 1 and Figure 2.

Sixth, we have investigated the effect of reducing the total error by a factor of three on the experimental measurement of the  $\nu_e$  flux while the best-estimate flux remains constant at the value quoted in ref. [1]. The currently allowed LMA and SMA solutions are not much affected by this hypothetical and optimistic error reduction, but the SMA is eliminated at  $3\sigma$  from the global solution with all the data included, as are also the active and sterile Just So<sup>2</sup> solutions. These results are apparent when comparing Figure 3 with Figure 1.

In summary, the CC measurement by SNO has not changed qualitatively the globally allowed solution space for solar neutrinos, although the CC measurement has provided dramatic and convincing evidence for neutrino oscillations and has strengthened the case for active oscillations with large mixing angles. These results are robust and does not depend sensitively on the details of the analysis assumptions. Future SNO measurements [25], including the day-night effect, the spectral energy distribution, and the neutral current to charge current ratio, will significantly reduce the allowed regions of parameter space [17]. The KamLAND [26] and BOREXINO [27] experiments will provide stringent diagnostics of different oscillation scenarios.

JNB acknowledges support from NSF grant No. PHY0070928. MCG-G thanks

the School of Natural Sciences in the Institute for Advanced Study (Princeton), where part of this work was carried out, for warm hospitality. CPG thanks the CERN theory division for their hospitality. MCG-G is supported by the European Union Marie-Curie fellowship HPMF-CT-2000-00516. This work was also supported by the Spanish DGICYT under grants PB98-0693 and PB97-1261, by the Generalitat Valenciana under grant GV99-3-1-01, and by the TMR network grant ERBFM-RXCT960090 of the European Union and ESF network 86.

## References

- [1] Q.R. Ahmad, et al., *Measurement of charged current interactions produced by  ${}^8\text{B}$  solar neutrinos at the Sudbury Neutrino Observatory*, submitted to *Phys. Rev. Lett.*.
- [2] B.T. Cleveland et al., *Measurement of the solar electron neutrino flux with the Homestake chlorine detector*, *Astrophys. J.* **496** (1998) 505.
- [3] W. Hampel et al. (GALLEX Collaboration), *GALLEX solar neutrino observations: results for GALLEX IV*, *Phys. Lett. B* **447** (1999) 127.
- [4] J.N. Abdurashitov et al. (SAGE Collaboration), *Measurement of the solar neutrino capture rate with gallium metal*, *Phys. Rev. C* **60** (1999) 055801 [astro-ph/9907113]; V. Gavrin (SAGE Collaboration), *Solar neutrino results from SAGE*, in *Neutrino 2000*, Proc. of the XIXth International Conference on Neutrino Physics and Astrophysics, 16–21 June 2000, eds. J. Law, R.W. Ollerhead, and J.J. Simpson, *Nucl. Phys. Proc. Suppl.* **91** (2001) 36.
- [5] M. Altmann et al. (GNO Collaboration), *GNO solar neutrino observations: results for GNO I*, *Phys. Lett. B* **490** (2000) 16; E. Bellotti et al. (GNO Collaboration), *First results from GNO*, in *Neutrino 2000*, Proc. of the XIXth International Conference on Neutrino Physics and Astrophysics, 16–21 June 2000, eds. J. Law, R.W. Ollerhead, and J.J. Simpson, *Nucl. Phys. Proc. Suppl.* **91** (2001) 44.
- [6] Y. Fukuda et al. (Super-Kamiokande Collaboration), *Measurements of the solar neutrino flux from Super-Kamiokande's first 300 days*, *Phys. Rev. Lett.* **81** (1998) 1158; Erratum **81** (1998) 4279; *Constraints on neutrino oscillation parameters from the measurement of day-night solar neutrino fluxes at Super-Kamiokande*, *Phys. Rev. Lett.* **82** (1999) 1810; Y. Suzuki (Super-Kamiokande Collaboration), *Solar neutrino results from Super-Kamiokande*, in *Neutrino 2000*, Proc. of the XIXth International Conference on Neutrino Physics and Astrophysics, 16–21 June 2000, eds. J. Law, R.W. Ollerhead, and J.J. Simpson, *Nucl. Phys. Proc. Suppl.* **91** (2001) 29.
- [7] P. Creminelli, G. Signorelli and A. Strumia, *Frequentist analyses of solar neutrino data*, *JHEP* **0105**, 052 (2001) [hep-ph/0102234].
- [8] J.N. Bahcall, P.I. Krastev and A.Yu. Smirnov, *Solar neutrinos: global analysis and implications for SNO*, *JHEP* 0105(2001)015 [hep-ph/0103179].
- [9] J.N. Bahcall, M.H. Pinsonneault and S. Basu, *Solar models: current epoch and time dependences, neutrinos, and heliosiesmological properties*, *Astrophys. J.* **555** (2001)(to be published) [astro-ph/0010346].
- [10] J.F. Beacom and S.J. Parke, *On the normalization of the neutrino-deuteron cross section* [hep-ph/0106128].
- [11] M. C. Gonzalez-Garcia, M. Maltoni, C. Peña-Garay and J.W.F. Valle, *Global three-neutrino oscillation analysis of neutrino data*, *Phys. Rev. D* **63** (2001) 033005 [hep-ph/0009350].

- [12] D. Dooling, C. Giunti, K. Kang and C.W. Kim, *Matter effects in four-neutrino mixing*, *Phys. Rev.* **D 61** (2000) 073011; C. Giunti, M.C. Gonzalez-Garcia and C. Peña-Garay, *Four-neutrino oscillation solutions of the solar neutrino problem*, *Phys. Rev.* **D 62** (2000) 013005.
- [13] G.L. Fogli, E. Lisi and D. Montanino, *Matter-enhanced three-flavor oscillations and the solar neutrino problem*, *Phys. Rev.* **D 54** (1996) 2048.
- [14] A. Gouvea, A. Friedland and H. Murayama, *The dark side of the solar neutrino parameter space*, *Phys. Lett.* **B 490** (2000) 125.
- [15] G.L. Fogli and E. Lisi, *Standard solar model uncertainties and their correlations in the analysis of the solar neutrino problem*, *Astropart. Phys.* **3** (1995) 185 with updated uncertainties as discussed in G.L. Fogli, E. Lisi, D. Montanino and A. Palazzo, *Three-flavor MSW solutions of the solar neutrino problem*, *Phys. Rev.* **D 62** (2000) 013002.
- [16] M.C. Gonzalez-Garcia and C. Peña-Garay, *Four-neutrino oscillations at SNO*, *Phys. Rev.* **D 63** (2001) 073013.
- [17] J.N. Bahcall, P.I. Krastev and A.Yu. Smirnov, *SNO: predictions for ten measurable quantities*, *Phys. Rev.* **D 62** (2000) 93004.
- [18] S. Nakamura, T. Sato, V. Gudkov and K. Kubodera, *Neutrino reactions on the deuteron*, *Phys. Rev.* **C 63** (2001) 034617.
- [19] M. Butler, J.-W. Chen and X. Kong, *Neutrino-deuteron scattering in effective field theory at next-to-next-to-leading order*, *Phys. Rev.* **C 63** (2001) 035501.
- [20] I.S. Towner, *Radiative corrections in neutrino-deuterium scattering*, *Phys. Rev.* **C 58** (1998) 1288.
- [21] A. McDonald and H. Robertson, private communications.
- [22] M. Apollonio et al., *Limits on neutrino oscillations from the CHOOZ experiment*, *Phys. Lett.* **B 466** (1999) 415.
- [23] R.S. Raghavan, *Solar neutrinos—from puzzle to paradox*, *Science* **267** (1995) 45.
- [24] P.I. Krastev and S.T. Petcov, *On the vacuum oscillation solutions of the solar neutrino problem*, *Phys. Rev.* **D 53** (1996) 1665.
- [25] A.B. McDonald (SNO collaboration), *The Sudbury Neutrino Observatory project*, *Nucl. Phys.* **B 77** (Proc. Suppl.) (1999) 43; G.T. Ewan, W.F. Davidson and C.K. Hargrove (SNO Collaboration), *The Sudbury Neutrino Observatory—an introduction*, *Physics in Canada* **48** (1992) 112; SNO Collaboration, *The Sudbury Neutrino Observatory*, *Nucl. Instrum. Meth.* **A 449** (2000) 172.

- [26] P. Alivisatos et al. (the KamLAND collaboration), *The KamLAND proposal*, Stanford-HEP-98-03; A. Piepke (KamLAND Collaboration), *KamLAND: A reactor neutrino experiment testing the solar neutrino anomaly*, in *Neutrino 2000*, Proc. of the XIXth International Conference on Neutrino Physics and Astrophysics, 16–21 June 2000, eds. J. Law, R.W. Ollerhead and J.J. Simpson, *Nucl. Phys.* **B** **91** (Proc. Suppl.), 99.
- [27] G. Alimonti et al. (BOREXINO collaboration), *Science and Technology of BOREXINO: a real time detector for low energy solar neutrinos* [hep-ex/0012030].